Fabrication of transparent ceria films by spray deposition without post firing

Ruwan Gallage · Atsushi Matsuo · Tomoaki Watanabe ·
Nobuhiro Matsushita · Masahiro Yoshimura

Abstract Most of the existing methods of crystalline ceria (CeO$_2$) films preparation consume much time and cost. Here we describe a straightforward and relatively cost-effective method of CeO$_2$ films preparation that involves direct spray deposition process on glass substrates at moderate temperatures (300–400 °C) using cerium acetate precursor in mixture of water and ethanol. X-ray diffraction analysis of obtained films revealed that they were polycrystalline, at least for a certain extent, with cubic fluorite structure and showed the existence of nanocrystallites. Scanning electron microscopic analysis showed that the films were crack-free and consists of nanocrystalline (<10 nm) ceria. Furthermore, the film showed high transparency in the visible and near-infrared region with calculated optical band gap (E_g) value of 3.06–3.08 eV. The film formation mechanism to obtain the transparent film has also been proposed.

Keywords Cerium oxide · Film · Spray deposition · Optical properties · Transparent film

1 Introduction

Cerium oxide is a striking material in various applications, including a solid oxide fuel cell electrolyte, automotive catalyst, barrier layers in superconductive materials, optical devices, etc. [1–4]. It forms the fluorite structure with the oxygen four coordinate and the cerium eight coordinate; one cerium atom is surrounded by eight oxygen atoms with space group Fm3m. Pure CeO$_2$ is pale yellow in color most likely due to the Ce(IV)–O(II) charge transfer transition [5].

There are different techniques that have been applied for the preparation of ceria films; e.g. CVD process [6] rf sputtering [7], sol-gel and spin coating [8]. However, the former techniques are time consuming and high cost processes. Sol-gel and spin coatings technique can be used to prepare dense and optical quality films [8, 9]. However it needs viscous precursor solutions (polymer content is quit high) and drying should be followed before each successive coating of precursor. Therefore, multi-step processes required repeatedly to obtain a thicker film [10]. Furthermore post heat treatments above 600 °C are essential for sol-gel method for remove all the organic compounds those used as polymerizing agents and densification or microstructure manipulation of the film [8, 10]. On the other hand spray deposition (pyrolysis) is one of the effective processing techniques that can be used to prepare ceramics films at low temperature [11, 12]. This process is essentially a continuous and allows facile fabrication of large-area coatings both dense and porous at a low cost. It offers advantages of controlling the composition and microstructure of the film, which is an asset for eventual technological applications especially to obtain film of desired thickness. Unlike many other film deposition techniques, this method is straightforward and relatively cost-effective particularly in terms of equipment costs. Furthermore, it does not require high quality substrates or chemicals because it usually involves atomizing a precursor solution to an aerosol, which is then directed to a heated substrate where a film is formed. Spray deposition technique has been employed for fabrication of ceria films with or without post heat treatments at high temperatures [11–14]. Elidrissi et al. [12] have prepared

R. Gallage · A. Matsuo · T. Watanabe · N. Matsushita ·
M. Yoshimura (✉)
Materials and Structures Laboratory,
Tokyo Institute of Technology,
4259 Nagatsuta,
Yokohama, Japan
e-mail: yoshimura@msl.titech.ac.jp

crystalline ceria films using aqueous cerium precursor solutions at the substrate temperature above 400 °C and below that temperature the film was almost amorphous. Furthermore, Petrova et al. [11] have reported the application of spray deposited technique for fabrication of crystalline ceria film at the substrate temperature almost above the 350°C using citric or tartaric complexes as starting solution. Here we report a preparation process of transparent ceria films without any complexing agents even at low deposition temperature (~300 °C) using cerium acetate {Ce(OOCCH$_3$)$_3$} as cerium source. The mechanism of the formation of the transparent CeO$_2$ film by this method has also been proposed.

2 Experimental procedure

Precursor solution was prepared by dissolving the cerium (III) acetate monohydrate, Ce(OOCCH$_3$)$_3 \cdot$H$_2$O (Kanto Chem. Co., Japan) salt in distilled water and ethanol mixture with the volume ratio 70:30. After stirring about 36 h at room temperature, transparent colourless solution was obtained without any precipitation. The concentration of the prepared solution was 0.02 mol/l.

The spray deposition setup is mainly composed of following parts; a spray gun (LPH-50-042G, ANEST IWTA Co., Japan), temperature-controlling unit (FCK-11, FINE, Japan), air compressor (ANEST IWTA Co., Japan) and home-made cartridge-heating unit (Fig. 1). Corning #7059 (20×20×1 mm) glass plates were used as substrates.

The substrate plates were cleaned with distilled water and acetone prior to the spray deposition process. Each cleaned plate was placed on the cartridge heater and was fixed onto it followed by heating up to predetermined temperature. The distance of ~20 cm was set between the substrate and the spray gun nozzle (inner diameter is 0.4 mm). Film samples were made by applying 10, 15 and 20 numbers of spray cycles of which each cycle consisted
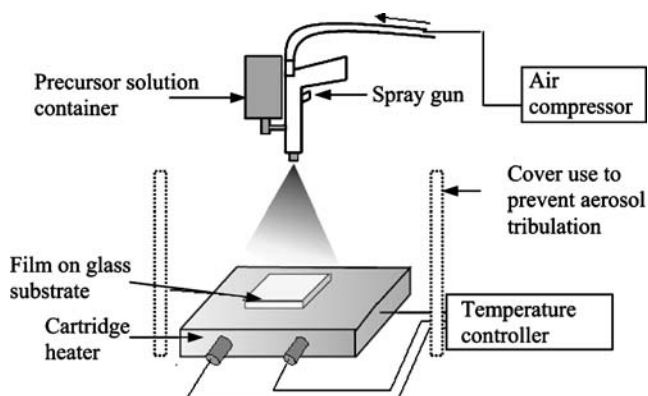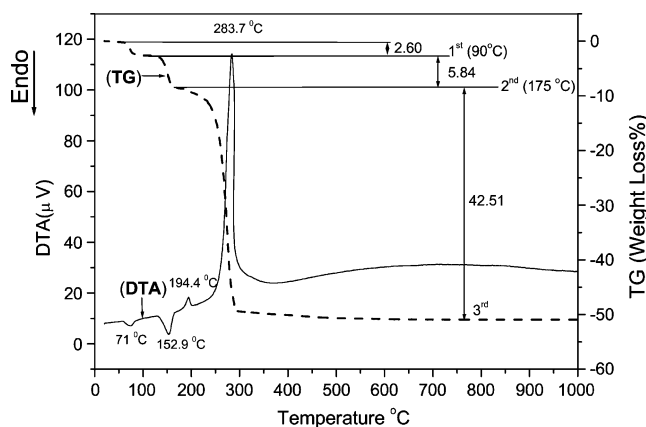

Fig. 1 Schematic diagram of spray deposition

Fig. 2 Thermal analysis curves for Ce(OOCCH$_3$)$_3 \cdot$H$_2$O decomposition in air

of 6–8 s of spray time. To restore the substrate temperature approximately 1 min interval between consecutive cycles was allowed. Spray deposition was proceeded at different substrate temperatures (300, 350, 375 and 400 °C).

Decomposition behavior of the cerium salts was studied using thermogravimetry and differential thermal analysis (TG-DTA; Type-2020, MAC Science Co., Ltd., Tokyo, Japan). The resultant phases of the fabricated films were characterized by X-ray diffraction. A standard X-ray diffractometer (Model MXP^{3VA}, MAC Science Co., Japan) was used with CuK$_\alpha$ radiation at 40 kV and 40 mA. The crystallite sizes were estimated from the line broadening in the XRD patterns run at a scan rate of 0.5°/min using the Williamson–Hall method [15]. Assuming the absence of lattice strains, the average crystallite size (D) was calculated from the diffraction line broadening according to Scherrer equation: $D=0.9\lambda/\beta\cos\theta$, where β is the corrected broadening of the diffraction line measured at half of its maximum intensity (radians) and D the diameter of crystallite. λ and θ are the wavelength of the X-rays ($\lambda=$ 1.5406 Å) and diffraction angle respectively. β can be calculated using Warren's formula: $\beta^2 = \beta_m^2 - \beta_s^2$, where, β_m is the measured half-width and β_s is the half-width of a standard CeO$_2$ sample [16]. Film surfaces and thickness were observed using scanning electron microscope (SEM; S4000, Hitachi Co., Ltd., Japan). The optical transmittance characteristics were investigated in the wavelength region of 200–1,000 nm using Lambda 35 UV/VIS spectrometer (PerkinElmer Instruments LIC, USA).

3 Results and discussion

TG-DTA was carried out to study the decomposition behavior of the cerium acetate precursor and the results are shown in Fig. 2. The endothermic peaks at 71 and 152.9 °C are due to the dehydration while a exothermic

peak at 194.4 °C without mass loss can be attributed to the crystallization of amorphous cerium(III) anhydrous acetate [17]. The strong exothermic peak around 280 °C accompanied with a fast mass loss refers to the decomposition of anhydrous cerium acetate. The obtained weight loss (48.35%) for the decomposition of precursor from the thermal gravimetric curve was almost similar to the calculated theoretical weight loss (48.65%) for cerium oxide formation. The data of thermal analysis clearly indicate that the decomposition occurs at about 280 °C. The absence of peaks after the major peak in DTA curve (at ∼280 °C) indicates that the crystallization process also occurs at the same temperature together with the decomposition process.

3.1 Structural analysis and surface morphology

X-ray diffraction (XRD) patterns of deposited films at the substrate temperature of 300, 350, 375 and 400 °C are shown in Fig. 3. All the peaks present in the XRD patterns were indexed as the standard crystallized CeO_2 with the fluorite structure [18, 19]. Neither intermediate nor other impurity phases were detected.

Selection of precursors also plays an important role especially in ceramic film fabricated by spray deposition process, since the minimum fabrication temperature that give a oxide film with lesser amount of polymeric components(cheating agents) depends on the decomposition temperatures of precursor salt and polymers. In the most case of ceria film fabricated by polymeric precursor showed higher decomposition temperature above 600 °C [20] than that of cerium acetate (Fig. 2) which used in this work without any cheating agent. Aqueous solutions of $CeCl_3$ and $Ce(NO_3)_3$ have been used by Elidrissi et al. [12] to prepare crystalline ceria, however, rather higher temperatures (∼400°C) were needed to prepare the crystalline film under their experimental conditions. In our method, nanocrystalline ceria could be obtained
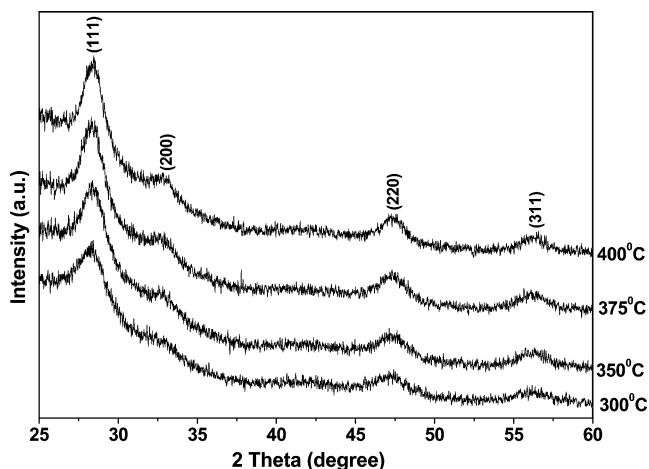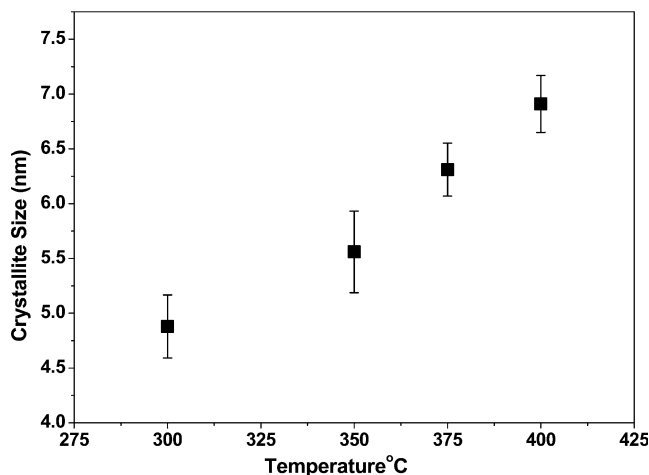

**Fig. 4** Effect of substrate temperature on crystallite size of ceria

even at 300°C (Fig. 3) using cerium acetate aqueous solution. Furthermore, DTA-TG analysis (Fig. 2) also confirmed the formation of crystalline ceria directly below 300 °C (∼280 °C).

The XRD results indicate the broadening of diffraction lines for all the film samples, which may be attributed to the small crystallites size (nanocrystallizes). The calculated crystallites sizes for the films prepared at the substrate temperatures between 300 and 400 °C were 5–7±0.3 nm (Fig. 4). Similar feature of XRD line broadening has been observed for the nanocrystalline ceria prepared at low temperatures in elsewhere [21, 22, 23]. However from our results it is difficult to conclude that these films are fully crystalline since all the processes were conducted below 400 °C.

The surface of the prepared ceria film prepared at different substrate temperature exhibits rounded particles and free of cracks (Fig. 5). The cross sectional images (Fig. 6) show that the films are dense and have adequate adhesion. High magnification SEM images revealed that the ceria films consist of nanosize particles less than 10 nm in size. This size estimation is rather consistent with the crystallites size calculated using XRD line broadening. It is confirmed that the broad peaks appeared in the XRD patterns are mainly due to the presence of nanosize ceria crystallites in the films.

Further analysis of the XRD data using window based "CellCalc" software [24] for the ceria film prepared at 400 °C showed that the calculated lattice parameter (a_o) is 0.5427±0.0002 nm. This value is similar to that of the ceria films prepared by spray deposition (0.542 nm) [12]. However this is slightly higher than the lattice parameter value mentioned in JCPDS data (0.5411 nm). Previous studies on the lattice expansion in ceria nanoparticles prepared at low temperature were mainly based on the reduction of Ce^{4+} to Ce^{3+} and formation of oxygen vacancies [25–27], exclusively for smaller crystallites with less than 10 nm. Nonetheless, the lack of crystallinity due to low temperature preparation (≤400 °C) and OH^- ions incorpora-

Fig. 3 XRD patterns for ceria film fabricated on glass substrates at different substrate temperatures

Fig. 5 SEM images of ceria films prepared at 300 and 400 °C on glass substrates (total spray time=8×10 s)
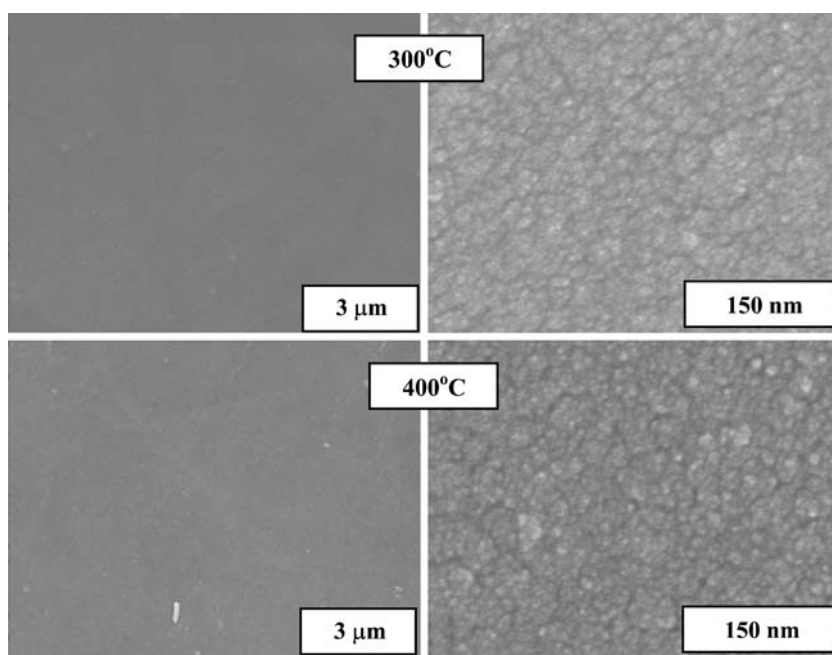
tion in the fluorite lattice (lattice defects) are also like to have an effect on the expansion of the lattice. Two OH^- ions are needed to substitute one O^{2-} ion. One of these OH^- ions could substitute into O^{2-} site and the other might be located in interstitial site in the fluorite structure. Under these circumstances the films have no strong colour with contrasting "blue" indicating the absence of CeO_{2-x} products with mixed valencies of Ce^{4+} and Ce^{3+} (the blue colour is

originated due to such CeO_{2-x} containing Ce^{3+} [28]). Our previous studies on nanocrystals of ceria–zirconia solid solutions under hydrothermal conditions suggested that the lattice expansion of the fluorite related phases below 400 °C is cause by the OH^- ions [22]. This expansion is brought by the lattice defects in both anion and cation sublattices thus the reduction of cation is not always the cause for the lattice expansion.
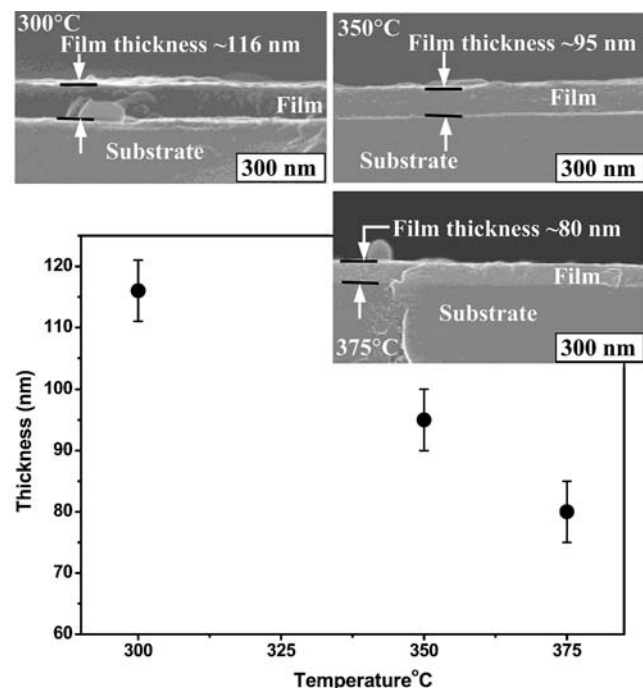
3.2 Dependency of film thickness on substrate temperature

The variation of the film thickness on the substrate temperature was studied. The results suggest that the film thickness is decreased by increasing the substrate temperature as shown in Fig. 6. Raising the substrate temperature will increase rate of the solvent evaporation that subsequently reduces the droplet size. It is known that several forces such as gravitational, thermophoretic and Stokes are acting on the droplets during their migration towards the heated substrate. The strongest thermophoretic forces are generated near the substrate, where the temperature gradient is largest, pushing the small droplets away from the substrate. This is because surrounding gas molecules of the hotter side of the droplet are rebound with higher kinetic energy than those from the cooler side. This effect reduces the number of droplets reached onto the substrate in one spray cycle [29], decreasing the film thickness.

3.3 Optical properties of ceria films

Cerium oxide films are widely used in optical single-layer or multilayer system due to its high transmission in the
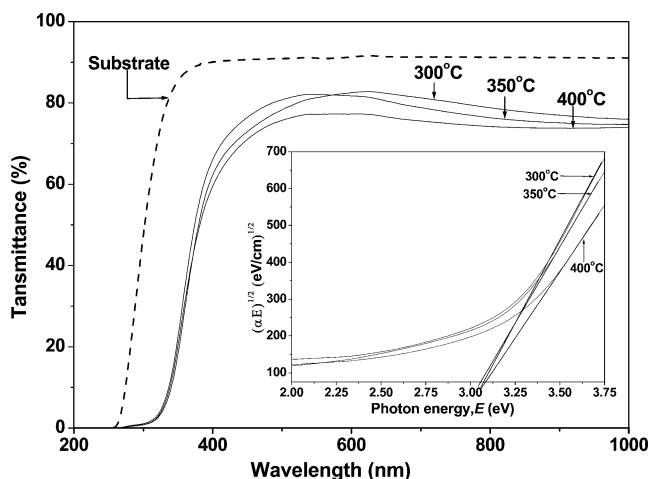

Fig. 6 Variation of the film thickness with substrate temperature and cross sectional images of prepared films

Fig. 7 Optical transmission spectra and the graphs of $(\alpha_a E)^{1/2}$ verses photon energy, E for ceria films fabricated at different temperatures on corning glass substrates

visible and infrared regions together with very sharp optical absorption edge. Ceria films prepared on the Corning glass substrate at different substrate temperatures were analyzed for their transmittance in the visible and infrared region with reference to air using UV/VIS spectrometer as shown in the Fig. 7 (left). All the ceria films on glass substrates showed high transparency with more than 70% transmittance(~85% with respect to the glass substrate) in both visible and infrared regions. The optical property of the absorbance in the UV region of ceria suggests that it can be used as a good candidate for UV absorbing materials.

The optical band gap (E_g) was determined from the absorption coefficient for an indirect allowed transition by $(\alpha_a E)^{1/2} = A(E - E_g)$, where α_a is absorption coefficient or constant, E is the photon energy ($h\nu$) and A is a constant [4]. The variation of $(\alpha_a E)^{1/2}$ with photon energy (E) is shown in Fig. 7 (right). The optical band gap for each film fabricated at different temperatures was obtained by linear extrapolation towards zero absorption of the $(\alpha_a E)^{1/2}$ vs E plot since $(\alpha_a E)^{1/2}$ is linear above E_g (Fig. 7) for an indirect allowed transition.

The values of the optical band gap for all ceria films are ~3.06–3.08 eV. These values are comparable to the values of ceria films prepared by sol-gel method at 450 °C (3.03–3.07 eV) [4]. However optical band gap values for the spray deposited ceria films are smaller than those of the films prepared by magnetron sputtering at about 800 °C (E_g ~3.30 eV) [7] as well as by physical vapour deposition ($3.15 < E_g < 3.25$) [30]. Both sol gel deposited films and spray deposited films at low temperatures have smaller grain size with random orientation [9, 31]. Therefore, it can be suggested that the higher concentration of grain boundaries is responsible for the broadening of absorption edge and apparent shift towards the lower energy of the

optical band gap. Patsalas et al. [32] observed the correlation of the optical band gap with their microstructures and composition of nanocrystalline (grain of 8–40 nm) ceria film prepared by electron-beam evaporation (EBE) at room temperature and 950 °C. Further, they showed that E_g is decreased by increasing the Ce^{3+} ion content in EBE film.

3.4 Proposed film formation mechanism by spray deposition

There are several processes that occur either sequentially or simultaneously during spray deposition process, such as evaporation of residual solvent, spreading of the droplet, pyrolytic decomposition of the salt, nucleation and growth of the oxide particles to consolidate into the film, etc. Understanding these processes would help to improve the film quality.

In the present work, we introduce a model for the film formation by concerning the above factors. In film formation mechanism there are two steps (Fig. 8); step 1, arrival of the droplet towards the substrate, and step 2, the formation, growth and densification of the film as illustrated in Fig. 8. Here we take only the formation of AO_2 film using precursor solution containing AX (X-acetate) into consideration so as to simplify the discussion. There are several factors that can affect on the film formation such as solubility of salt, physical properties of solvents, substrate temperature and etc. Among them solubility of the salt is an important factor to be considered in step 1. If the solubility is low, salt begins to precipitate within the droplets just before hitting it to the heated substrate due to evaporation of the solvents. It may lead to either non-continuous deposition or accumulation of non-sticking powder on the substrate [33]. Cerium acetate shows high solubility in water and ethanol, thus it may not precipitate within the droplet before hitting the substrate, resulting the formation of dense film on the substrate without any powder particles up to 400 °C as shown in Figs. 5 and 6. However, we
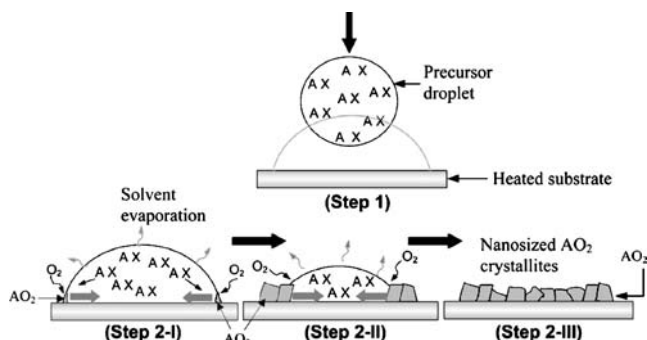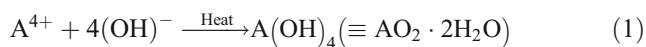

Fig. 8 Schematic illustration for the film formation mechanism by spray deposition

observed that easily removable non-sticking powders on the surface when the substrate temperature was above 400 °C. In the second step, the impacted droplet spreads on the heated substrate and then starts the spontaneous processes of oxidation of Ce^{3+} to Ce^{4+} and heterogeneous nucleation of $A(OH)_4$($\equiv AO_2 \cdot 2H_2O$, oxide hydrate) at the solid (substrate), liquid and gas interface (periphery of the droplet), as shown in Fig. 8 (2-I) then change to AO_2. This oxide nucleation on the substrate from the solution might be similar to the spinel formation in ferrite plating [34]. The nucleation occurs towards the center until all the solvents evaporate (2-II). The expected reactions occur in these process are as follows.

$$A^{4+} + 4(OH)^- \xrightarrow{\text{Heat}} A(OH)_4 (\equiv AO_2 \cdot 2H_2O) \qquad (1)$$

$$AO_2 \cdot 2H_2O \xrightarrow{\text{Heat}} AO_2 \qquad (2)$$

While the evaporation of solvents, oxide hydrate and AO_2 oxide are continuously formed on the substrate (reactions 1 and 2). At the end of the process well-adhered nanocrystalline dense AO_2 film is directly formed on the heated substrate [19, 35].

Sears et al. investigated the spray deposition mechanism of SnO_2 film, concluding that the film is grown from the vapour of droplets passing very close to the hot substrate in a manner of chemical vapour deposition [36]. However, the authors have not considered the spreading of the droplets on the substrate, which significantly contribute to the film growth in the spray pyrolysis process. Beckel et al. [33] have recently reported the film formation mechanism of spray pyrolysis considering the precursor precipitation occur within the droplet before impact it to the substrate due to the saturation condition by evaporating the solvents. Additionally, they described the film formation process, which was done by spreading the droplet and stacking the precipitates on the heated substrate. In their model, however, decomposition of precursor, neuleation and growth of the films were not taken into consideration.

4 Conclusions

Here we show a successful method of transparent cerium oxide film preparation even at 300 °C and propose a film formation mechanism for the process. It involves on-site spray deposition using cerium precursor solution (cerium acetate) without any chelating agents at moderate temperatures (≤400 °C). The fabricated films on glass substrate have high optical transparency (more than 70%) relative to the air. The optical band gap (E_g) of these films is relatively low and it is in the rage of 3.06–3.08 eV. Film fabrication at

moderate temperatures enhances the adhesion of film due to onsite nucleation and growth. Overall mechanism of the process consists of two steps as droplet movements followed by the formation of the film. The technique is very effective for making optically passive nanostructured (crystallites size < 10 nm), dense cerium oxide film.

References

1. H. Inaba, H. Tagawa, Solid State Ion. **83**, 1 (1996)
2. A. Trovarelli, Cat. Rev. **38**, 439 (1996)
3. X. Xiong, D. Winkler, Physica C: Superconductivity **336**, 70 (2000)
4. N. Ozer, Sol. Energy Mater. Sol. Cells **68**, 391 (2001)
5. M. Mogensen, N.M. Sammes, G.A. Tompsett, Solid State Ion. **129**, 63 (2000)
6. N. Zu, N. Murayama, W. Shin, I. Matsubara, S. Kanzaki, Jap. J. Appl. Phys. **43**, 6920 (2004)
7. S. Guo, H. Atwin, S.N. Jacobsen, K. Jkrendahl, U. Helmersson, J. Appl. Phys. **77**, 5369 (1995)
8. T. Suzuki, I. Kosacki, H.U. Anderson, Solid State Ion. **151**, 111 (2002)
9. T. Suzuki, I. Kosacki, V. Petrovsky, H.U. Anderson, J. Appl. Phys. **91**, 2308 (2002)
10. R.W. Schwartz, T. Schneller, R. Waser, C. R. Chimie **7**, 433 (2004)
11. N.L. Petrova, R.V. Todorovsk, D.S. Todorovsky, Solid State Ion. **177**, 613 (2006)
12. B. Elidrissi, M. Addoua, M. Regragui, C. Monty, A. Bougrine, A. Kachouane, Thin Solid Films **379**, 23 (2000)
13. J.L.M. Rupp, A. Infortuna, L.J. Gauckler, Acta Mater. **54**, 1721–1730 (2006)
14. J.L.M. Rupp, L.J. Gauckler, Solid State Ion. **177**, 2512 (2006)
15. B.D. Cullity, *Elements of X-ray Diffraction* (Addison-Wesley, California, 1978)
16. Standard Reference Materials. SRM 674b, CeO_2 (fluorite structure) internal standard reference material for quantitative analysis by x-ray powder diffraction. National Bureau of Standards, Washington, DC (2000)
17. T. Arii, A. Kishi, M. Ogawa, Y. Sawada, Anal. Sci. **17**, 875 (2001)
18. Powder Diffraction Files. PDF 34-0394, JCPDS – International center for diffraction data (1998)
19. R. Gallage, A. Matsuo, T. Fujiwara, T. Watanabe, N. Matsushita, M. Yoshimura, J. Am. Ceram. Soc. (in press)
20. B. Rousseau, S. Phok, L. Ortega, N. Guibadj, T. Wegelius, S. Morlens, P. Odier, F. Weiss, J. Eikmeyer, J. Eur. Ceram. Soc. **25**, 2185 (2005)
21. C. Ho, J.C. Yu, T. Kwong, A.C. Mak, S. Lai, Chem. Mater. **17**, 4514 (2005)
22. A. Ahniyaz, T. Watanabe, M. Yoshimura, J. Phys. Chem. B **109**, 6136 (2005)
23. A.S. Deshpande, M. Niederberger, Microporous Mesoporous Mater. **101**, 413 (2007)
24. H. Miyura, *"CellCalc" Ver. 1.51: Windows program to calculate unit cell parameters* (University of Hokkaido, Japan, 2003)
25. F. Zhang, S.-W. Chan, J.E. Spanier, E. Apak, Q. Jin, R.D. Robinson, I.P. Herman, Appl. Phys. Lett. **80**, 127 (2002)
26. S. Tsunekawa, K. Ishikawa, Z.-Q. Li, Y. Kawazoe, A. Kasuya, Phys. Rev. Lett. **85**, 3440 (2000)
27. V. Perebeinos, S.W. Chan, F. Zhang, Solid State Commun. **123**, 295 (2002)

28. T. Sata, M. Yoshimura, Bull. Tokyo Inst. Technol **84**, 13 (1968)
29. D. Peredins, O. Wiihelm, S.E. Pratsinis, L.J. Gauckler, Thin Solid Films **474**, 84 (2005)
30. G.C. Granqvist, *Hand book of Inorganic Electrochromic Materials* (Elservier, The Netherlands, 1995)
31. F. Wooten, *Optical properties of solids* (Academic Press, New York, 1972)
32. P. Patsalas, S. Logothetidis, C. Metaxa, Appl. Phys. Lett. **81**, 466 (2002)
33. D. Beckel, A. Dubach, A.R. Studart, L.J. Gauckler, J. Electroceram. **16**, 221 (2006)
34. M. Abe, Electrochim. Acta **45**, 3337 (2000)
35. A. Matsuo, R. Gallage, T. Fujiwara, T. Watanabe, M. Yoshimura, J. Electroceram **16**, 533 (2006)
36. W.M. Sears, M.A. Gee, Thin Solid Films **165**, 265 (1988)